Minerals Engineering 123 (2018) 167–172

Contents lists available at ScienceDirect

Minerals Engineering

journal homepage: www.elsevier.com/locate/mineng

Analysis of key mixing parameters in industrial Wemco mechanical flotation cells

T.C. Souza Pinto[a], A.S. Braga[a,c], L.S. Leal Filho[a,c], D.A. Deglon[b,*]

[a] Instituto Tecnológico Vale – ITV, 31, Juscelino Kubitschek Av., Ground Floor, Bauxita, 35400-000 Ouro Preto, MG, Brazil
[b] Centre for Minerals Research – CMR, University of Cape Town, Private Bag, Rondebosch 7700, South Africa
[c] University of São Paulo, Polytechnic Engineering School, Mining and Petroleum Department, 2373 Prof. Mello Moraes Av., 05508-900 São Paulo, SP, Brazil

ARTICLE INFO

Keywords:
Flotation cells
Hydrodynamics
Residence time distribution
Mixing

ABSTRACT

Flotation performance in mechanical cells is strongly influenced by hydrodynamics. Hydrodynamics is driven by the action of the impeller which is responsible for mixing in the cell. This paper evaluates key mixing parameters in three industrial Wemco mechanical flotation cells (#144, #164, #190; 14.2, 28.3, 42.5 m^3). Residence time distributions, circulation times, impeller pumping capacities, impeller Flow numbers and power intensities are presented. RTD studies are based on LiCl tracer measurements. RTD studies showed that the #190, #164 & #144 behave as 2.1–2.4, 1.2 and 1.0 tanks in series respectively. Circulation times for the #164 and #144 were much shorter than the #190. The #190 and #164 had the highest pumping capacities. Dimensionless Flow numbers varied from 0.12 to 0.22. Iron losses by entrainment of fine particles (< 45 μm) were higher in the #164, due to the higher intensity of mixing.

1. Introduction

Mechanical flotation cells are the work-horses of the flotation industry and, despite competition from a large variety of alternative flotation technologies, are still responsible for the bulk of world flotation. The performance of mechanical flotation cells is strongly influenced by hydrodynamics. Hydrodynamics is a broad term used to describe fluid flow, but generally refers to the bulk or macroscopic flow of fluid in the vessel. Hydrodynamics is largely driven by the action of the impeller which establishes a flow pattern, or average path of the bulk fluid flow. Flow patterns are governed by vessel characteristics, such as size and shape, and impeller properties such as geometry and rotational speed. Fluid leaves the impeller in axial, radial and tangential fluid jets which carry kinetic energy, in the form of fluid flow, into the bulk cell where they ultimately decay into turbulence and circulate back to the impeller. Historically, hydrodynamics in flotation has been described using a range of dimensionless numbers and key hydrodynamic parameters; e.g. power intensity, impeller tip speed, Power number, Froude number, tank-turnover time and Air flow number. Hydrodynamics is responsible for mixing which is important in mechanically agitated flotation cells. The mixing intensity must be suitable for creating favorable conditions for efficient solids suspension and gas/solids dispersion. Here, most mechanical flotation cells operate in the turbulent environment with a magnitude of $Re \sim 10^6$ (Schubert and Bischofberger, 1978; Harris, 1986). Mixing affects micro turbulence, generally associated with eddies generated in the vicinity of impeller region, which is responsible for the performance of flotation sub processes. Hydrodynamics and mixing are ultimately driven by the action of the impeller which must be optimized to promote three well established zones inside the equipment: 1. Turbulent zone (collision and attachment), 2. Quiescent zone (separation); 3. Froth zone (Schubert and Bischofberger, 1978; Massey et al., 2012; Tabosa et al., 2016).

The impeller used in industrial mechanical flotation cells has a different geometry to those used in conventional mixing processes such as Rushton turbines, propellers and pitched blade turbines. Harris (1986) reported that flotation cells generally have an aspect ratio (impeller to tank diameter) in the range of 0.25–0.5 while Arbiter et al. (1976) reported this range as between 0.25–0.64. McCabe et al. (2005) stated that the ratio of impeller to tank diameter suitable for gas dispersion should be around 0.25. Numerous studies have investigated the effect of impeller speed on flotation parameters such as the superficial gas velocity, bubble size and rate constant (Gorain et al., 1995, 1996; Schubert, 1999; Deglon et al., 1999; Deglon, 2005). These studies have often concluded that an increase in the impeller speed leads to an increase in the flotation rate for fine particles. The effect of agitation intensity on flotation performance also differs for fine and coarse particles as investigated by Ahmed and Jameson (1985), Schubert and Bischofberger (1978), and Schubert (1999). There are not many

* Corresponding author.
E-mail address: David.Deglon@uct.ac.za (D.A. Deglon).

https://doi.org/10.1016/j.mineng.2018.03.046
Received 5 January 2018; Received in revised form 27 March 2018; Accepted 28 March 2018
Available online 13 April 2018
0892-6875/

List of symbols

Re	Reynolds number [–]	τ	spatial time [T]
RTD	residence time distribution [T]	V	tank volume [L^3]
t_{circ}	circulation times [T]	Q	volumetric flow rate [L^3/T]
Q_b	impeller pumping capacity [L^3/T]	t_{avg}	average residence time [T]
N_Q	impeller Flow number [–]	S	standard deviation
N	impeller speed [1/T]	C_∞	maximum tracer concentration [M/L^3]
D	impeller diameter [L]	ε_g	gas holdup [%]
T	tank diameter [L]	wt	solid concentration [%]
		V_{up}	upward pulp superficial velocity flux [L/T]
		ρ	slurry density [M/L^3]

literature studies which investigate mixing in industrial mechanical flotation cells. This study investigates mixing in three different industrial Wemco mechanical cells in terms of the residence time distribution, circulation time, impeller pumping capacity, impeller Flow number and power intensity.

2. Background

Mechanical flotation cells are often characterized as continuous stirred tank reactors (CSTRs). Industrial mechanical flotation cells deviate from perfectly mixed CSTRs through short-circuiting and/or stagnant zones (Lelinski et al., 2002; Yianatos et al., 2008). This non-ideal behavior affects particle-bubble contacting through factors such as poor solids suspension or gas dispersion. Residence time distribution (RTD) studies are important for evaluating the quality of mixing and determining deviations from ideal CSTR behavior (Fogler, 1999; Patwardhan et al., 2003). Mixing aims to reduce the degree of non-homogeneity in the vessel (Uhl and Gray, 1966; Chhabra and Richardson, 1999). Flotation cells have three phases, solid-liquid-gas, and the extent of mixing influences contact between all phases. This affects parameters such as mixing patterns, rate of mixing, mixing times, power consumption and scale-up (Coulson and Richardson, 1999). There have been numerous hydrodynamic flotation studies in flotation cells of various size, from laboratory up to industrial cells (Arbiter, 2000). Here, researchers have found clear discrepancies in results. Perry and Green (2007) note that the difference between small and large scale vessels leads to significant differences in blending and circulation times, which tends to be higher in larger vessels. This is corroborated by Arbiter et al. (1976). A recirculation pattern also tends to develop in larger vessels resulting in a similar behavior to CSTRs (Perry and Green, (2007).

The flotation impeller is often modelled as a pump with a partly open case. Here, fluid is continuously transferred upwards to the top of the tank and then recirculated back to the impeller (Arbiter et al., 1976). The impeller's effectiveness in this regard is often evaluated by its pumping capacity (Q_b) or by the dimensionless Flow number (N_Q), as shown in Eq. (1). In the laminar and turbulent regime, the flow number is typically constant. For the transitional regime, the flow number is dependent of the impeller Reynolds number and the fluid properties. A high flow number (N_Q) indicates a high impeller pumping capacity and liquid circulation intensity thus generating better mixing (Joshi et al., 1982; Tatterson, 1991; Nienow, 1997).

$$N_Q = \frac{Q_b}{ND^3} \tag{1}$$

The extent of mixing is often evaluated in terms of the circulation time or tank turnover time which are affected by the impeller pumping capacity (Yianatos et al., 2008). A short circulation or tank turnover time means good dispersion of air and solids throughout the cell (Tatterson, 1991; Nienow, 1997; Deglon et al., 2000; Yianatos et al., 2008). The mean circulation time or tank turnover time is calculated as the effective volume of the flotation tank divided by the impeller pumping capacity. The reciprocal of this quantity is referred to as the circulation intensity (Deglon et al., 2000; Nelson and Lelinsk, 2000). The mixing time can also be determined by RTD (tracer) methods, as the time required for the disappearance of most of the tracer (typically 95%). The mixing time is usually in the range of 3–5 times the circulation time (Khang and Levenspiel, 1976; Joshi et al., 1982; Nienow, 1997; Carletti et al., 2016). However, some researchers have found the ratio of the mixing time to the circulation time to be slightly lower, in the range of 2–2.3 (Uhl and Gray, 1966). RTD studies can be performed by different techniques such as soluble tracer, conductivity or colorimetric methods (Nienow, 1997; Takenaka et al., 2005). The presence of gas in the flotation cell usually leads to an increase of the critical impeller speed and an increase in the circulation time (Joshi et al., 1982; Perry and Green, 2007). Wemco 1 + 1 brochures have this information for different cell sizes but for water only i.e. no gas or solids.

3. Experimental

RTD studies were performed in three industrial Wemco mechanical flotation cells of different size, as shown in Table 1. It is interesting to note that the impeller diameter in these cells is higher than standard for Wemco 1 + 1 cells. The #144 cell has a #164 impeller diameter and so on. This is typical of industrial practice but means that the impeller must be operated at different speeds to those suggested in the Wemco brochure. The Wemco #190 cell operates in a circuit removing silica elements containing MgO such as olivine, pyroxenes and phlogopite for producing a final product for the cement industry (MgO < 5.5%). The circuit is fed with the tailings from a prior apatite flotation circuit. In this cell, RTD studies were conducted at three different impeller speed as the cell has a variable speed driver. The other two cell models (#164 and #144) operate in reverse flotation iron ore circuits, removing silica components (mainly quartz). Prior to conducting RTD studies, the cells were thoroughly characterized for gas dispersion parameters such as gas hold up, bubble diameter and gas superficial velocity using probes as described by Yianatos et al. (2001) and Deglon et al. (2000).

The first flotation cell in each industrial bank was evaluated. The banks consisted of 4 #190 cells (phosphate tailings circuit), 4 #164 cells (iron ore rougher circuit) and 3 #144 cells (iron ore cleaner circuit). RTD studies were conducted by adding a tracer (LiCl) as a pulse in the flotation cell feed box. The amount of tracer added to each cell was fixed at a known concentration (ppm) accordingly to the tank volume. Samples of pulp were taken at set time intervals in the cell corner

Table 1
Flotation cells used for the RTD studies.

Wemco model	Duty[a]	Imp. Dia. (m)	Imp. speed (rpm)	Cell Vol. (m^3)	Gas Holdup (%)	SiO_2 Rec/cell (%)
#190	RG	0.990	130	42.5	8	11
			140		10	18
			154		12	21
#164	RG	0.889	155	28.3	14	42
#144	CL	0.762	175	14.15	11	40

[a] RG = Rougher; CL = Cleaner.

immediately below the froth. A top-bottom open/close sampler of 500 ml was used. The tracer concentration was determined by AAS. Feed, tail and concentrate flow rates and grades were determined and mass balanced by pertinent software (JKSimFloat). Table 2 shows the flotation cell geometry.

The impeller-tank (D/T) aspect ratio of 0.25 in the Wemco 1 + 1 brochure is corroborated by Arbiter et al. (1976) who noted that Wemcos have a small aspect ratio. The choice of a higher impeller-tank ratio and slower impeller speed in the industrial flotation cells suggests that bulk flow and mixing are prioritized over turbulence intensity, which requires smaller impellers at high speeds (McCabe et al., 2005). Another reason to use larger D/T ratios is where a high degree of solids suspension and shorter mixing times are required (Takenaka et al., 2005; Panneerselvam et al., 2008).

4. Results and discussion

4.1. Residence time distribution

Fig. 1 shows the residence time distributions for the three flotation cells. From the RTD curves it is clear that in general the flotation cells behave as a series of well mixed tanks.

The RTD function E(t) was used for determining the average/mean residence time (t_{avg}) from Eq. (2) and the number of ideal tanks in series (n) from Eqs. (3) and (4) for the tanks in series model. Here, t is the time, σ^2 is the variance and τ is the expected residence time or space time calculated from the volumetric flow rate ($\tau = V/Q$).

$$t_{avg} = \int_0^\infty t.\, E(t)dt \tag{2}$$

$$E(t) = \frac{t^{n-1}e^{\frac{-tn}{\tau}}}{\left(\frac{\tau}{n}\right)^n (n-1)!} \tag{3}$$

$$n = \frac{t_{avg}^2}{\sigma^2} \tag{4}$$

The RTD results are summarized in Table 3. The #190 behaves as 2.1–2.4 tanks in series. As the impeller speed increases, the number of ideal tank in series decreases slightly. The #164 and #144 behave as 1.2 and 1.0 tanks in series respectively, indicating that the smaller cells are well mixed. The feed rate of the flotation circuit for the #190 remained constant for all tested impeller speeds. Nevertheless, slightly differences were found in the expected residence time due to changes in the gas holdup. The expected residence time for the #190 was around 5.0 min and decreased with increasing impeller speed. The expected residence times for the #164 and #144 were 3.7 min and 3.0 min respectively. The average residence times (t_{avg}) for the #164 and #144 were higher than the expected residence time while an opposite trend was found for the #190, where $\tau > t_{avg}$.

Lelinski et al. (2002) analysed RTD studies for various types of mechanical flotation cells. Here, Wemco cells were found to have the smallest deviation between the expected and average residence times. In this work, the #190 has a smaller average residence time than the expected residence time. This suggest that slurry remains in the cell for a shorter period, indicating either by-passing of slurry or dead zones in the cell. The #164 has a longer average residence time than the expected residence time, which is unusual and may be due to the measured flow rate. For the #144 both residence times are similar showing that the cell is well mixed.

Yianatos et al. (2015) presented results for the number of ideal tank in series for different types of large flotation cells (130 m^3). They concluded that the number of real cells ranged from 75% to 100% of the ideal tanks in series equivalent. For this study, results for the #190 show a large number of tanks in series (± 50% real to ideal) and much smaller average residence times than expected. From this it may be concluded that mixing inside the #190 can be improved, possibly by increasing the impeller speed. For the #164 and #144, the number of tanks in series is similar to the number of cells, again suggesting better mixing in the smaller cells.

Fogler (1999) noted that, from the ideal tank-in-series model, the standard deviation (σ) should be equal to the average residence time. The #190 has the highest deviation between t_{avg} and σ with the ratio (t_{avg}/σ) lying in the range 1.5–1.6. The #164 and #144 have ratios in the vicinity of 1.0, again confirming that these cells are well-mixed.

4.2. Circulation time

Yianatos et al. (2008) investigated the mixing performance of 130 m^3 self-aerated flotation cells. In their work, it was assumed a complete-mixed condition inside the tank when all the applied sensors (tracer detectors) spread out in the cell achieved a similar magnitude. The authors considered the time delay between the two sensors as the time length between the peaks of RTD response curves for each probe. They considered the geometrical aspects of the tank and sensor location to determine the impeller pumping capacity. Cheng et al. (2012) researching a semi-batch system made the same assumption, considering the well-mixed condition to be when the different probes in the cell reached a maximum tracer concentration.

Based on the data of Yianatos et al. (2008) and Cheng et al. (2012), this study considers the peak of the RTD curve to be an approximate indicator of the circulation time (t_{circ}). This data was used to determine the ratio between the experimental mixing time and the peak of the RTD curve. This ratio was found to be in the range of 2–3, which is similar to the ratio of the mixing to circulation times discussed in Section 2, suggesting that the circulation time is in the vicinity of the RTD peak. This is an assumption but seems reasonable given that one would expect the maximum tracer concentration to be achieved within one full tank turnover. RTD studies are relatively simple for a plant metallurgist to conduct, whereas measuring impeller pumping capacities in operating flotation cells is more complex. However, it should be noted that this method would give an estimate of the actual circulation time. Circulation times estimated from the RTD response curves for the flotation cells and corresponding data from the Wemco 1 + 1 brochure (water only) are given in Fig. 2.

The RTD circulation times for the #164 and #144 are much shorter than the #190. This is corroborated by Deglon et al. (2000), who noted that the tank turnover time increases with increasing cell size. The circulation time for water is much lower than the RTD circulation time, but follows the same trend with increasing cell size. This is probably due to the circulation times being estimated from the RTD peak and/or the impeller pumping capacity for water being significantly higher than for three-phase systems (Tatterson, 1991). Here, the gas and solids tend to damp both fluid flow and turbulence dissipation throughout the tank (Schubert, 1999). Cheng et al. (2012) and Joshi et al., (1982) noted that the gas holdup can reduce the liquid circulation velocity due to a reduction in power consumption in the presence of gas. The ratios of the RTD circulation times to the Wemco 1 + 1 brochure (water only) circulation times range from 1.7 to 3.1. These ratios are expected to be greater than 1 for reasons discussed previously. However, the ratios do suggest that the #164 is the most well-mixed cell and that the mixing is

Table 2
Flotation cell geometry.

Cell type	Wemco 1 + 1 Brochure. D_{imp} (m)	Tank diam.[a] (m)	Impeller aspect ratio	Impeller/ tank aspect ratio (Wemco 1 + 1)	Impeller/tank aspect ratio (industrial)
#144	0.660	2.76	1	0.24	0.28
#164	0.762	3.04	1	0.25	0.29
#190	0.889	3.62	0.92	0.25	0.28

[a] Wemco 1 + 1 cells are rectangular (tank diameter refers to cell length).

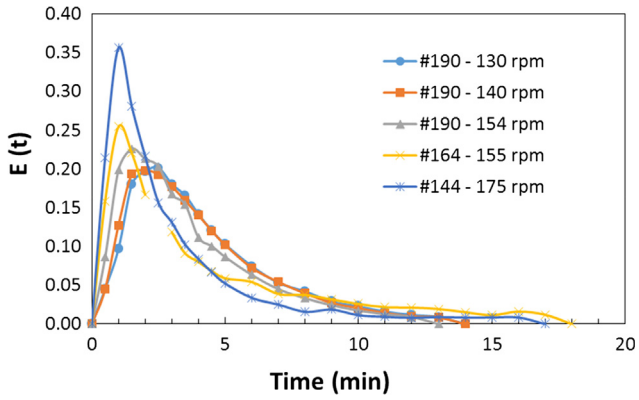

Fig. 1. RTD function for the three flotation cells.

Table 3
Residence time distribution results.

Wemco model	Imp. speed (rpm)	t_{avg} (min)	τ (min)	σ	τ/t_{avg}	No. ideal tank
#190	130	4.2	5.1	2.7	1.2	2.4
	140	4.1	5.0	2.7	1.2	2.3
	154	3.7	4.8	2.6	1.4	2.1
#164	155	4.6	3.7	4.2	0.8	1.2
#144	175	3.2	3.0	3.2	0.9	1.0

generally poor in the #190 at the lower impeller speeds.

The RTD response curves can be used for determining the mass fraction of tracer that exits the cell before the circulation time by mass balance using Eq. (5).

$$\int_0^\infty E(t)dt = 1 \tag{5}$$

Fig. 3 shows the results for the fraction of tracer exiting the tank up to the circulation time. The amount of tracer that exits the cell before the well mixed condition is considered to be the by-pass fraction and is estimated as the fraction that left the cell before the circulation time. Here, the #190 operating at 130 rpm has the highest by-pass fraction at around 30% while the #164 has less than half this by-pass fraction. This again suggests that #164 is the most well-mixed flotation cell. Yianatos et al. (2008) found a by-pass fraction of up to 9.4% for a 130 m^3 flotation cell but no information about the impeller speed and type was available.

4.3. Impeller pumping capacity

The impeller pumping capacity can be calculated from the circulation time using Eq. (6). The impeller pumping capacity (Q_b) and dimensionless Flow number (N_Q) data for the flotation cells are given in Table 4.

$$Q_b = \frac{V_{liq.}*(1-\varepsilon_g)}{t_{circ}} \tag{6}$$

The highest impeller pumping capacities are observed for the #190 (154 rpm) and #164, at around 25 m^3/min. The lowest value was found for the #144. As the aspect ratio D/T is quite similar for all cell models, a slightly increase in the impeller speed should lead to an increase in the impeller pumping capacity. The number of times that the pulp phase recirculates through the impeller can be estimated by the ratio of the average residence time to the circulation time. This lead to 2.5, 4.6 and 3.2 recirculation times for the #190, #164 and #144 respectively. Joshi et al. (1982) note that complete mixing is achieved after 5 recirculation times (Nienow, 1997), as corroborated by Yianatos et al. (2008). This again suggests that the #164 is a well-mixed cell.

The dimensionless Flow number (N_Q) results for the flotation cells vary from 0.12 to 0.22. The upward pulp superficial velocity flux (V_{up}) can be determined as the ratio of the cell cross sectional area and pumping capacity, as shown in Eq. (7).

$$V_{up} = \frac{Q_b}{A_{froth}} \tag{7}$$

The #164 and #144 cells operate in a circuit for the reverse flotation of iron ore. The measured water recovery for the #164 was 12.5% with an iron losses by entrainment (−45 μm) of around 30% while these numbers are 11% water recovery and 20% iron losses for the #144. The higher the water recovery the higher the iron losses, as corroborated by Lima et al. (2016). For the #190, which operates in a phosphate tailings circuit, entrainment is associated with CaO particles found in the froth phase. Here, froth depth (pulp level) affects water recovery and the consequent entrainment of fine particles. Nevertheless, it is worthwhile noting that the upward pulp superficial velocity flux velocity for the #164 is 56% higher than that for the #144. This may well be a contributing factor for the higher entrainment and is due to the higher impeller pumping capacity.

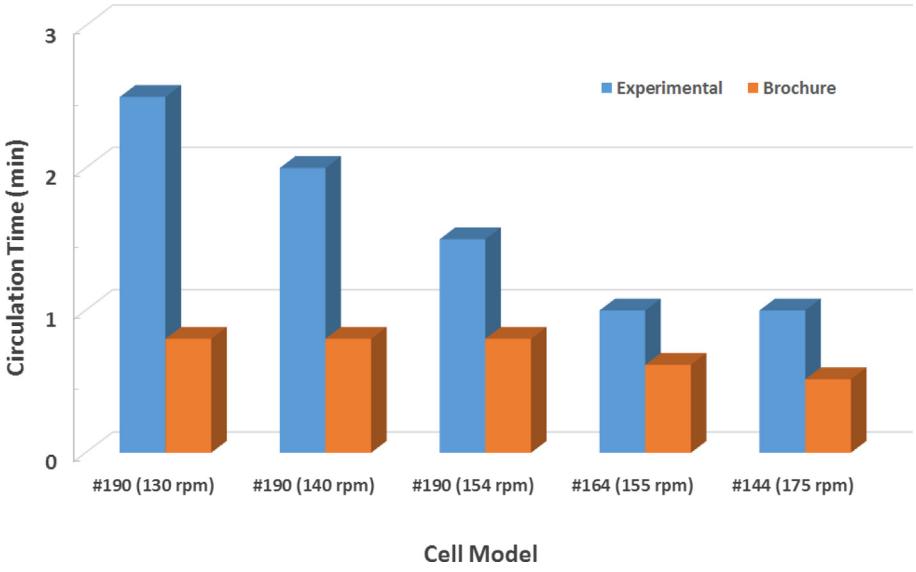

Fig. 2. Circulation time results.

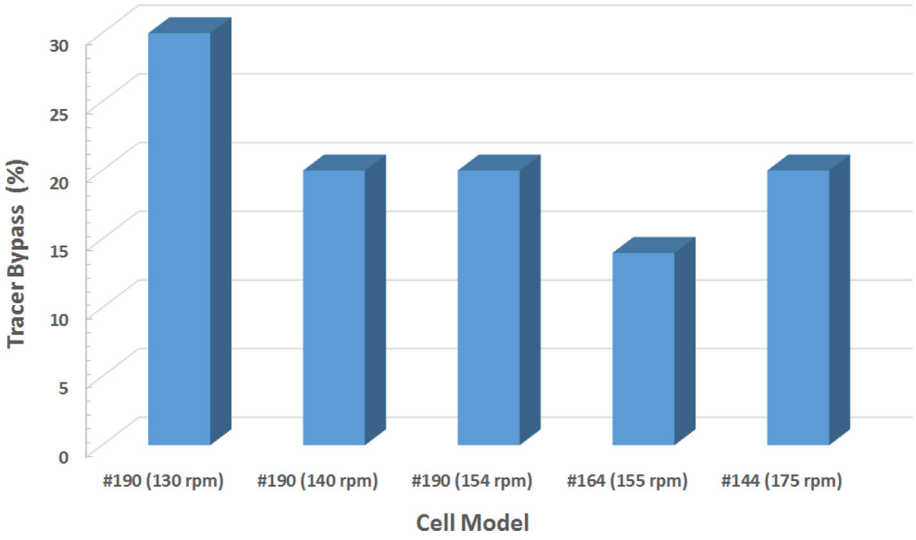

Fig. 3. Tracer by-pass results.

Table 4
Impeller pumping parameter results.

Cell model	#190			#164	#144
Impeller speed	154 rpm	140 rpm	130 rpm	155 rpm	175 rpm
Q_b, m^3/min	25.8	19.4	15.5	24.4	12.7
N_Q [–]	0.16	0.14	0.12	0.22	0.16
Eff. Cell vol., m^3	36.6	38.3	39.1	24.3	12.7
[a]Froth area, m^2	15.60			11.3	9.2
V_{up}, cm/s	2.7	2.1	1.6	3.6	2.3

[a] Data from Wemco 1 + 1 brochure.

4.4. Power intensity

As indicated in the experimental, the industrial flotation cells have larger impellers than standard for Wemco 1 + 1 i.e. higher D/T ratios. The power input in these cells was not measured but the power intensity (P/V) is proportional to $\rho N^3 D^5$. The proportional power intensities calculated from this correlation are given in Fig. 4.

Here, the magnitude of these numbers is lower than actual but trends will be comparable. Deglon et al. (2000) did a similar evaluation for the tank turnover time as the ratio of tank volume to ND^3. It is clear from Fig. 4 that the proportional power intensities in the industrial cells are higher than those for the standard Wemco. Here, the ratio of estimated power intensity to brochure power intensity is 1.4, 1.3 and 1.6 for the Wemco #190, #164 and #144 respectively. One cannot compare these power intensities directly, but this would suggest that #144 should have good mixing characteristics, as noted in previous sections.

5. Conclusions

Flotation performance in mechanical cells is strongly influenced by hydrodynamics. Hydrodynamics is largely driven by the action of the impeller, which is responsible for mixing in the cell. This paper evaluated key mixing parameters in three industrial Wemco mechanical flotation cells (#144, #164, #190). From this paper, one may conclude:

- Residence time distributions: RTD studies showed that the #190, #164 & #144 behave as 2.1–2.4, 1.2 and 1.0 tanks in series respectively. The tracer by-pass fraction up to circulation time ranged from 14% to 30%. RTD results indicate that mixing in the #190 can be improved.
- Circulation times: RTD estimated circulation times for the #164 and #144 were much shorter than the #190, at around 1 min compared to 2 min for the larger cell.

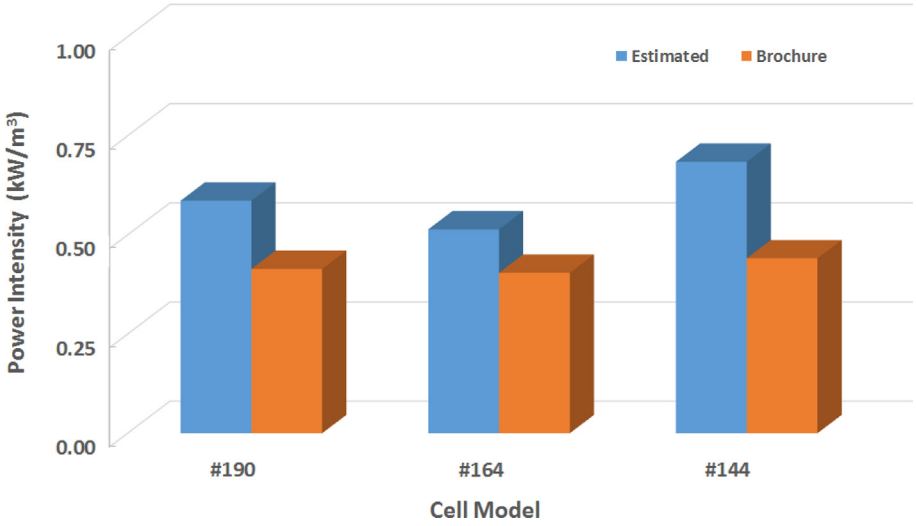

Fig. 4. Power intensity results (numbers given are not actual power intensities but proportional quantities.)

- Impeller pumping capacities: Results showed that the #190 (154 rpm) and the #164 had the highest pumping capacities at round 25 m^3/min.
- Impeller Flow numbers: Dimensionless Flow number varied from 0.12 to 0.22, which is lower than typical water-only values.
- Power intensities: The ratio of estimated power intensity to brochure power intensity were 1.4, 1.3 and 1.6 for the Wemco #190, #164 and #144 respectively.
- Entrainment: Results demonstrate iron losses by entrainment of fine particles (< 45 μm) are higher in the #164, which may be related to the higher intensity of mixing.

This study investigated mixing in industrial Wemco mechanical flotation cells. However, the analysis of mixing parameters presented in this study is considered applicable to other types of industrial mechanical flotation cells. In addition, this analysis may also be applicable to mixing in stirred tanks used in solid–liquid-gas applications. The assumption that the peak of the RTD curve is an approximate indicator of the circulation time may be a useful first estimate for plant metallurgists, as RTD studies are relatively simple to conduct.

Acknowledgements

The authors acknowledge the support of Valefert and Iron ore department from Vale S/A. Site personnel of Cajati and Brucutu assisted with the survey and their help is greatly appreciated.

References

Ahmed, N., Jameson, G.J., 1985. The effect of bubble size on the rate of flotation of fine particles. Int. J. Miner. Process. 14, 195–215.
Arbiter, N., Harris, C.C., Yap, R.F., 1976. The air flow number in flotation machine scale-up. Int. J. Miner. Process. 3, 257–280.
Arbiter, N., 2000. Development and scale-up of large flotation cells. Miner. Eng. 52 (3), 28–33.
Carletti, C., Montante, G., De Blasio, C., Pagliante, A., 2016. Liquid mixing dynamics in slurry stirred tanks based on electrical resistance tomography. Chem. Eng. Sci. 152, 478–487.
Cheng, D., Cheng, J., Li, X., Wang, X., Yang, C., Mao, Z., 2012. Experimental study on gas-liquid-liquid macro mixing in a stirred tank. Chem. Eng. Sci. 75, 256–266.
Chhabra, R.P., Richardson, J.F., 1999. Non-Newtonian Flow in the Process Industries. Butterworth-Heinemann, Oxford.
Coulson, J.M., Richardson, J.F., 1999. Coulson & Richardson's Chemical Engineering. Fluid flow, heat transfer and mass transfer, 6th ed. vol. 1 Butterworth-Heinemann, Oxford.
Deglon, D.A., 2005. The effect of agitation on the flotation of platinum ores. Miner. Eng. 18, 839–844.
Deglon, D.A., Egya Mensah, D., Franzidis, J.P., 2000. Review of hydrodynamics and gas dispersion in flotation cell on South African platinum concentrators. Miner. Eng. 13 (3), 235–244.
Deglon, D.A., Sawyerr, F., O'Connor, C.T., 1999. A model to relate the flotation rate constant and the bubble surface area flux in mechanical flotation cells. Miner. Eng. 12 (6), 599–608.
Fogler, H.S., 1999. Elements of Chemical Reaction Engineering, 3rd ed. Prentice Hall.
Gorain, B.K., Franzidis, J.P., Manlapig, E.V., 1995. Studies on impeller type, impeller speed and air flow rate in an industrial scale flotation cell. Part 2: effect on gas holdup. Miner. Eng. 8 (12), 1557–1570.
Gorain, B.K., Franzidis, J.P., Manlapig, E.V., 1996a. Studies on impeller type, impeller speed and air flow rate in an industrial scale flotation cell. Part 3: Effect on superficial gas velocity. Miner. Eng. 9 (6), 639–654.
Gorain, B.K., Franzidis, J.P., Manlapig, E.V., 1996b. Studies on impeller type, impeller speed and air flow rate in an industrial scale flotation cell. Part 4: Effect of bubble surface area flux on flotation kinetics. Miner. Eng. 10 (4), 367–379.
Harris, C.C., 1986. Flotation machine design, scale-up and performance. In: Somasundaran, P. (Ed.), Advances in Mineral Processing. SME.
Joshi, J.B., Pandit, A.B., Sharma, M.M., 1982. Mechanically agitated gas-liquid reactors, Review article number 7. Chem. Eng. Sci. 37 (6), 813–844.
Lelinski, D., Allen, J., Redden, L., Weber, A., 2002. Analysis of the residence time distribution in large flotation machines. Miner. Eng. 15, 499–505.
Khang, J.S., Levenspiel, O., 1976. New scale-up and design method for stirrer agitated batch mixing vessels. Chem. Eng. Sci. 31 (7), 569–577.
Lima, N.P., Souza Pinto, T.C., Tavares, A.C., Sweet, J., 2016. The entrainment effect on the performance of iron ore reverse flotation. Miner. Eng., 96–97, 53-58.
Massey, W.T., Harris, M.C., Deglon, D.A., 2012. The effect of energy input on the flotation of quartz in an oscillating grid flotation cell. Miner. Eng. 36–38, 145–151.
McCabe, W.L., Smith, J.C., Harriot, P., 2005. Unit Operation of Chemical Engineering, 7th ed. McGraw-Hill.
Nelson, M.G., Lelinsk, D., 2000. Hydrodynamics design of self-aerating flotation machines. Miner. Eng. 10–11, 991–998.
Nienow, A.W., 1997. On impeller circulation and mixing effectiveness in the turbulent flow regime. Chem. Eng. Sci. 52 (15), 2557–2565.
Panneerselvam, R., Savithri, S., Surender, G.D., 2008. CFD modeling of gas-liquid-solid mechanically agitated contactor. Chem. Eng. Res. Des. 86, 1331–1344.
Patwardhan, A.W., Pandit, A.B., Joshi, J.B., 2003. The role of convection and turbulent dispersion in blending. Chem. Eng. Sci. 58 (2003), 2951–2962.
Perry, R.H., Green, D.W., 2007. Perry's Chemical Engineering Handbook, 8th ed. McGraw-Hill.
Schubert, H., Bischofberger, C., 1978. On the hydrodynamics of flotation machines. Int. J. Miner. Process. 5, 132–142.
Schubert, H., 1999. On the turbulence controlled microprocesses in flotation machines. Int. J. Miner. Process. 56, 257–276.
Tabosa, E., Runge, K., Holtham, P., 2016. The effect of cell hydrodynamics on flotation performance. Int. J. Miner. Process. 156, 99–107.
Takenaka, K., Takahashi, K., Bujalski, W., Nienow, A., Paolini, S., Paglianti, A., Etchells, A., 2005. Mixing time for different diameters of impeller at a high solid concentration in agitated vessel. J. Chem. Eng. Sci. Jpn. 38 (5), 309–315.
Tatterson, G.B., 1991. Fluid mixing and gas dispersion in agitated tanks. McGraw-Hill.
Uhl, V.W., Gray, J.B., 1966. Mixing theory and practice. vol.1 Academic Press Inc., New York.
Wemco 1 + 1 Flotation machines brochure.
Yianatos, J., Bergh, L., Condori, P., Aguilera, J., 2001. Hydrodynamic and metallurgical characterization of industrial flottion banks for control purposes. Miner. Eng. 14 (9), 1033–1046.
Yianatos, J., Larenas, J., Moys, M., Diaz, F., 2008. Short time mixing response in a big flotation cell. Int. J. Miner. Process. 89, 1–8.
Yianatos, J., Bergh, L., Vinnett, L., Panire, I., Diaz, F., 2015. Modelling of residence time distribution of liquid and solid in mechanical flotation cells. Miner. Eng. 78, 69–73.